Heterotrophs are key contributors to nitrous oxide production in mixed liquor under low C-to-N ratios during nitrification - batch experiments and modelling

Domingo Felez, Carlos; Pellicer i Nàcher, Carles; Petersen, Morten S.; Jensen, Marlene Mark; Plósz, Benedek G.; Smets, Barth F.

Published in:
Biotechnology and Bioengineering

Link to article, DOI:
10.1002/bit.26062

Publication date:
2017

Document Version
Peer reviewed version

Heterotrophs are key contributors to nitrous oxide production in mixed liquor under low C-to-N ratios during nitrification – batch experiments and modelling

Author list

Carlos Domingo-Félez[1], Carles Pellicer-Nàcher[1], Morten S. Petersen[1], Marlene M. Jensen[1], Benedek G. Plósz[1], Barth F. Smets[1]*

[1]Department of Environmental Engineering, Technical University of Denmark, Miljøvej 113, 2800 Kgs. Lyngby, Denmark

* Corresponding author:

Barth F. Smets, Phone: +45 4525 1600, Fax: +45 4593 2850, E-mail: bfsm@env.dtu.dk

Running title: N_2O production in nitrifying batch experiments: heterotrophic and autotrophic contributions.

Abstract

Nitrous oxide (N_2O), a by-product of biological nitrogen removal during wastewater treatment, is produced by ammonia-oxidizing bacteria (AOB) and heterotrophic denitrifying bacteria (HB). Mathematical models are used to predict N_2O emissions, often including AOB as the main N_2O producer. Several model structures have been proposed without consensus calibration procedures. Here, we present a new experimental design that we used to calibrate AOB-driven N_2O dynamics of a mixed culture. Even though AOB activity was favoured with respect to HB, oxygen uptake rates indicated HB activity. Hence, rigorous experimental design for calibration of autotrophic N_2O production from mixed cultures is essential. The proposed N_2O production pathways were examined using five alternative process models confronted with experimental data inferred. Individually, the autotrophic and heterotrophic denitrification pathway could describe the observed data. In the best-fit model, which combined two denitrification pathways, the heterotrophic contribution to N_2O production was stronger than the autotrophic. Importantly, the individual contribution of autotrophic and heterotrophic to the total N_2O pool could not be unambiguously elucidated solely based on bulk N_2O measurements. NO data availability will increase the practical identifiability of N_2O production pathways.

Keywords: Nitrous oxide, Batch, Nitrification, Denitrification, Model

1. Introduction

Nitrous oxide (N_2O) is known as both a stratospheric ozone depleter and a greenhouse gas with 300 times higher radiative forcing than carbon dioxide (Stocker et al., 2013). N_2O is emitted during biological nitrogen removal and its emission factors are highly variable between wastewater treatment plants (WWTPs) (0.01-3.3% $N_2O_{emitted}/TN_{removed}$) (Ahn et al., 2010). Moreover, the carbon footprint of a WWTP is highly sensitive to N_2O emissions (Gustavsson and Tumlin, 2013), as an N_2O emission factor of 1% can increase its carbon footprint by 50% (Monteith et al., 2005).

N_2O is biologically produced during wastewater treatment by ammonium oxidizing bacteria (AOB) and heterotrophic denitrifying bacteria (HB). AOB can produce N_2O as a by-product of hydroxylamine oxidation (NH_2OH) or by nitrite (NO_2^-) reduction. As an obligate intermediate during nitrate (NO_3^-) reduction, N_2O can also be produced by HB (Law et al., 2012). The three pathways are commonly known as nitrifier nitrification (NN), nitrifier denitrification (ND) and heterotrophic denitrification (HD), respectively. Certain wastewater constituents such as dissolved oxygen (DO) and NO_2^- have been identified as key variables affecting N_2O dynamics (Kampschreur et al., 2009; Schreiber et al., 2012). However, other variables such as inorganic carbon content, known to affect nitrification rates (Jiang et al., 2015; Torà et al., 2010), have shown contradictory results with respect to N_2O (Khunjar et al., 2011; Peng et al., 2015a). Hence, the metabolic regulation of N_2O production is still under study (Perez-Garcia et al., 2014). Identifying the individual contribution of each pathway is critical for the design of N_2O mitigation strategies.

One way to elaborate on the individual contributions of the pathways is through N_2O process models. Several N_2O models have been proposed for one or two of the aforementioned N_2O production pathways (Guo and Vanrolleghem, 2013; Ni et al.,

2013a) with the final goal of mitigating its emissions. Models vary based on the true substrate considered for AOB (NH_3 vs. NH_4^+), a reaction's electron donor, or whether substrate inhibition is considered (Pan et al., 2013; Spérandio et al., 2016). How to mathematically describe these effects will impact the structural identifiability of model parameters (Dochain and Vanrolleghem, 2001).

Calibration of N_2O models typically rely on the same data series as N-removing models (DO, NH_4^+, NO_2^-, NO_3^-, COD) and additionally N_2O (Guo and Vanrolleghem, 2013; Ni et al., 2011). The type and quality of experimental data will affect the practical identifiability of model parameters (Dochain and Vanrolleghem, 2001). Literature for N_2O-associated parameters shows large variability for similar processes. For example, the AOB affinity for NO_2^- during autotrophic denitrification in nitrifying biomass has been reported from 0.14 to 8 mgN/L (Kampschreur et al., 2007; Schreiber, 2009). Similarly, for the same model, a wide range of autotrophic NO affinity constants has been used, from 0.004 to 1 mgN/L (Mampaey et al., 2013; Spérandio et al., 2016). Variations can arise from considering different microbial communities, model assumptions, quality of data or the calibration procedure selected.

Depending on the system, AOB or HB have been considered to be the main contributor to the total N_2O production (Itokawa et al., 2001; Ni et al., 2013a). ND and HD occur under similar DO and NO_2^- concentrations, thus leading to possible interferences between autotrophic and heterotrophic N_2O production (Shen et al., 2015; Wu et al., 2014). However, under certain operating conditions, the contribution of a pathway can be considered negligible, thus allowing for more accurate model calibrations. Experiments can be therefore specifically designed to study the autotrophic contribution to the total N_2O production pool from mixed liquor biomass. Nitric oxide (NO) is the direct precursor of N_2O for the three pathways, and even though it is included in most

N_2O models (Ni et al., 2011; Ni et al., 2014) few studies have focused on quantifying and describing NO emissions (Kampschreur et al., 2007; Schreiber et al., 2009), which has been shown to be a useful tool to calibrate N_2O models (Pocquet et al., 2016).

In this study, we assess to what extent batch experiments – designed to assess N_2O dynamics under nitrifying conditions from a mixed culture biomass from a typical BNR plant – allow for calibration of N_2O models. Specifically, without assuming prior knowledge of the main N_2O producing pathway, our objective was to:

- Identify what model structures are capable of describing N_2O production of mixed liquor during batch tests at varying substrate concentrations.
- Quantify the individual contribution of the main biological N_2O-producing pathways to the total modelled N_2O production.
- Elucidate challenges encountered during calibration of N_2O models with combined pathways.

2. Materials and Methods

2.1. Batch reactor configuration.

Batch experiments were performed in a 3L PYREX glass vessel (Bellco Glass Inc., USA), with 4 side ports used for pH, DO and N_2O microsensors, and inflow/outflow gas (Supporting Information (SI), Figure S1). The inlet and outlet gas flow was set at 60 mL/min with gas flow meters. Oxic and anoxic conditions in the reactor were obtained by air and N_2 supplied through a bubble diffuser. Aeration and mixing were controlled using a Labview (National Instruments, Austin, USA) routine. The DO and temperature data, (CellOx 325, WTW, Germany) and pH (SenTix41, WTW, Germany) was continuously logged at 0.017 Hz. Liquid N_2O concentrations were measured with Clark-type microsensors (N2O-R, Unisense A/S, Aarhus, Denmark). Gaseous N_2O concentrations were measured with an infrared gas analyzer (T320, Teledyne, USA).

Photometric test kits were used to analyse N-substrates (1.14752, 1.09713, 1.14776, Merck KGaA, Darmstadt, Germany). Biomass content (MLSS, MLVSS) was measured in triplicates according to APHA(APHA et al., 1999). Alkalinity was measured by titration after addition of sulphuric acid (APHA et al., 1999).

2.2.Batch tests.

Mixed liquor from a full-scale wastewater treatment plant (Lynetten, Copenhagen, Denmark) was sampled over a period of three months (May-July 2012). Mixed liquor was aerated overnight and the biomass concentration adjusted to 2-3 gVSS/L with aerated clarified wastewater before experiments. After two days of experimentation the biomass was discarded to prevent significant changes in biomass composition (Torà et al., 2010). The biomass composition was calculated thermodynamically (SI_1). Biomass samples for DNA extraction were taken for every new experiment (n = 8). Details on the qPCR quantification procedure can be found elsewhere (Terada et al., 2010) (SI_2).

Two sets of experiments were performed while aeration was kept constant. Instantaneous extant substrate loadings of 1-3 mgN/gVSS were designed to mimic typical plant loading conditions, which produce a representative description of the parent system (Ellis et al., 1996). In the first set of experiments (i) solely NH_4^+ was spiked at incremental concentrations (1-8mgN/L). NH_4^+ removal was monitored off-line via liquid analysis and online by observing DO drops (Table SII). In the second set of experiments (ii), again NH_4^+ spikes (3-5mgN/L) were made and when nearing NH_4^+ depletion a NO_2^- or NO_3^- spike (2mgN/L) was made, monitoring responses in liquid and gas phase. Experiments allowed for nitrogenous concentration changes at both high and low DO concentrations (DO = 6.5 – 0.2 mg/L), providing useful information regarding substrate affinities and growth rates and covering a wide range of potential N_2O

producing scenarios. Experiments were conducted and repeated the day after on consecutive weeks.

Heterotrophic activity was monitored during an anoxic experiment (iii) where N_2 was supplied instead of air under NO_3^- excess and no organic carbon addition. NO_3^- reduction was assumed to occur fed on hydrolysed products originated from biomass decay as no organic substrate was added. Simultaneously, NH_4^+ would be released and accumulate in the bulk phase.

To determine N_2O and O_2 mass transfer coefficients, stripping and reoxygenating experiments (iv) were performed separately at the same batch conditions in preaerated clarified wastewater (Eq. 1) (Garcia-Ochoa and Gomez, 2009). Liquid phase N_2O measurements were used to estimate net N_2O production rates as previously described (Domingo-Félez et al., 2014) (Eq. 2).

$$N_2O_{liq\,(t)} = N_2O_{liq\,(t=0)} \cdot e^{(-k_L a_{N_2O} \cdot t)} \text{ (mgN/L)} \qquad \text{(Eq. 1)}$$

$$N_2O\ \text{Prod. Rate}_i = \frac{\Delta N_2O_{liq\_i}}{\Delta t} + k_L a_{N_2O} \cdot N_2O_{liq_i} \text{ (mgN/L·min)} \qquad \text{(Eq. 2)}$$

2.3.Model description and calibration: NH_4^+, NO_2^-, NO_3^-, DO.

NH_4^+ to NO_3^- conversion was described by a 2-step nitrification model (Table SIII). First, AOB oxidize NH_4^+ to NH_2OH followed by its oxidation to NO_2^-. Subsequently NOB oxidize NO_2^- to NO_3^-. Heterotrophic denitrification was included as a 4-step process with NO_2^-, NO and N_2O as intermediates (Hiatt and Grady, 2008). Hydrolysis of particulates and ammonification were simplified into one hydrolytic process following biomass decay as no particulate N or soluble organic N data was available at the beginning of the experiments (Table SIV). Rates were not dependent on inorganic carbon as it was in excess during the experiments (5.8-6.0 mM HCO_3^-).

The simulation model was implemented in AQUASIM 2.1(Reichert, 1998).

The objective of the following calibration procedure was to fit DO, NH_4^+, NO_2^- and NO_3^- data. First, physico-chemical parameters (k_La) were estimated from experiments (iv). Second, nitrification was evaluated by experiments (i) and (ii). The measured OUR_{max} were used to estimate the NH_4^+ affinity (K_{NH4}^{AOB}), and the NH_4^+ oxidation rates at varying DO to estimate the DO affinity ($K_{O2,AMO}^{AOB}$) (SI_3). Then, oxic hydrolysis was evaluated against heterotrophic aerobic growth in experiments (i) and (ii) when reduced nitrogenous species were absent. Anoxic hydrolysis was assessed under anoxic conditions in experiment (iii). Finally, maximum growth rates (μ_{AOB}^{AMO}, μ_{NOB}) were estimated from NH_4^+ removal followed by NO_2^- removal and NO_3^- accumulation from experiments (ii). The rest of parameter values describing nitrification and denitrification were taken from published literature (Table SV). The biomass composition was modelled throughout the experiments to account for decay processes.

After good fits of DO and profiles of NH_4^+, NO_2^- and NO_3^- were achieved, the N_2O producing model structures (Tables S4) were calibrated.

2.4.Model description and calibration: N_2O.

The objective of implementing different N_2O model structures was to investigate what model structure, with accepted parameters, can describe the experimental data. Two model structures for AOB driven N_2O production were evaluated. The nitrifier denitrification (ND) pathway considers the consecutive reduction of NO_2^- to NO and N_2O as two processes. The model structure chosen in this study considers DO inhibition, and NH_2OH is modelled as the electron donor (Ni et al., 2011). The nitrifier nitrification (NN) pathway considers a 2-step NH_2OH oxidation over NO to NO_2^-. A

fraction of NO is reduced to N_2O with NH_2OH as the electron donor independent of DO levels (Ni et al., 2013a). Finally, N_2O can also be produced as an intermediate of heterotrophic denitrification in the 4-step model (HD) (Hiatt and Grady, 2008). Every step in the HD pathway considers independently easily biodegradable organic substrate as electron donor coupled with DO and NO inhibitions. Parameter values from two different denitrifying activated sludge systems (SRT = 3 and 10 days) (Hiatt and Grady, 2008; Schulthess et al., 1994) have been used regularly to describe HD (Table SVI). Because the aim of the experiments was to study the autotrophic N_2O production, both parameter subsets were considered throughout the study to avoid biases from the possible heterotrophic contribution: HD_a and HD_b.

Five different AOB-HB pathway combinations were tested to evaluate what model structures best describe the experimental N_2O data (Table I). Three scenarios consider a single N_2O production pathway: in scenarios NN and ND only nitrifier nitrification or nitrifier denitrification produce N_2O, while HD is modelled as a 2-step denitrification directly reducing NO_2^- to N_2 (i.e. no chance of heterotrophic N_2O production). Scenario HD considers only N_2O production through a 4-step denitrification process. Two scenarios, NN-HD and ND-HD, consider the combination of an autotrophic (either nitrifying nitrification or denitrification) with the heterotrophic pathway (Ni et al., 2011; Ni et al., 2013a). Differently from other comparative studies both autotrophic and heterotrophic pathways are considered without any prior assumption of the main producer (Spérandio et al., 2016). A multiple-pathway AOB model was not considered as the assumptions for the ND pathway make it incompatible with the 4-step denitrification model (Pocquet et al., 2016). The continuity for all the model structures was numerically evaluated following Hauduc et al. (2010) (Hauduc et al., 2010).

For each pathway, only certain parameters are specific to describe N_2O production. For the AOB-associated pathways (NN, ND), only parameters not affecting directly NO_2^- production were first considered: η_{AOB} and K_{NO}^{AOB} for NN and η_{AOB}, K_{NO}^{AOB}, K_{NO2}^{AOB} and $K_{i,O2}^{AOB}$ for ND (Table III). The high number of parameters describing each denitrification step (5) does not allow individual parameter estimation. Consequently, a sensitivity analysis based on the relative-relative function was used to avoid calibration of insensitive parameters in the three pathways. During calibration, the lower and upper limits were set to ± 50% from their original literature values.

Parameter estimation was performed by minimizing the sum of the squared errors weighted by their standard deviations. The likelihood measured of each fit was evaluated following Mannina et al. (2011), where an overall model efficiency (E_i) value of 1 corresponds to a perfect fit and tends zero for large errors (Eq. 3) (Mannina et al., 2011), where $\alpha_j$corresponds to each data series and $M_{j,i}$ and $O_{j,i}$ to modelled and observed points.

$$E_i = \sum_j^n \alpha_j L(\theta_i/Y_j) = \frac{1}{N}\sum_j^n \alpha_j \cdot \exp\left(-\frac{\left(\sum(M_{j,i}-O_{j,i})^2\right)^2}{\left(\sum(O_{j,i}-\bar{O}_{j,i})^2\right)^2}\right) \quad \text{(Eq. 3)}$$

In addition, the RMSE was calculated. The contribution of each individual process to the N_2O and NO concentration at any time was calculated by multiplying each process rate (P_i) with its stoichiometric coefficient (v_{ij}). The sum of all terms corresponds to the net production/consumption of the state variable (S_j) (Eq. 4).

$$S_{net\_prod\_j} = \sum_i (P_i \cdot v_{ij}) \qquad \text{(Eq. 4)}$$

Uncertainty analysis was done following Sin et al. (2010) by randomly sampling K_{NO}^{AOB} and K_{NO}^{HB} (0.02 ± 90% mgN/L).

3. Results

3.1.Oxygen uptake and hydrolysis during autotrophic batch experiments.

Experiments (i) and (ii) started with NH_4^+ and DO excess, reaching first DO followed by NH_4^+ limitation. DO reached limiting but never truly anoxic conditions (0.2-0.4 mg DO/L). NO_2^- accumulated shortly and was consumed simultaneously with NH_4^+ until depletion, upon which the DO concentration rapidly increased to pre-spike levels. NO_3^- accumulated to levels similar to the NH_4^+ added, indicating complete nitrification of NH_4^+ (Figure 1, left).

Because of the low amount of substrate added a simplified model structure not including biomass growth was first considered. However, in the absence of NH_4^+ or NO_2^- and at constant aeration DO never reached saturation, indicating an additional oxygen uptake process (Figure 1, right). Thus the model had to include processes producing biodegradable carbon from biomass decay. As no other organic source was present, the heterotrophic aerobic growth was responsible for the continuous oxygen uptake. Hence, hydrolysis affects DO availability even during short batch tests.

Under anoxic conditions hydrolytic processes also release biodegradable carbon and NH_4^+. Experimental and modelling results from the anoxic experiment (iii) showed agreement of ammonification and NO_3^- reduction (Figure S2).

3.2.N_2O production during autotrophic batch experiments.

During experiments (i), after NH_4^+ spikes N_2O increased slowly at high DO and sharply when reaching DO < 0.5 mg/L, and decreasing after NH_4^+ depletion and consequent DO increase (Figure S3). Experiments (ii) were used to investigate the effect of DO, followed by NO_2^- or NO_3^- addition, on N_2O production during NH_4^+ oxidation. After adding NH_4^+, N_2O concentration gradually increased until DO became limiting, which

rapidly increased its production (Figure 2A, time < 20 min). A NO_3^- spike added to promote heterotrophic denitrification during DO limiting conditions did not increase the net N_2O production compared to a sole NH_4^+ spike (Figure 2B). On the other hand, NO_2^- addition at low oxygen concentrations and in the presence of NH_4^+ drastically increased the N_2O production (Figure 2C). These results are in agreement with literature where NO_2^- showed a larger impact on N_2O production compared to NO_3^- under endogenous conditions (Wu et al., 2014). The net N_2O produced after an NH_4^+ (or NH_4^+ followed by NO_3^-) spike was approximately 0.9% of the nitrogen oxidized, while 1.9% of the nitrogen oxidized was converted to N_2O when NH_4^+ was spiked followed by NO_2^- .

3.3.Model calibration for oxygen and nitrogenous substrates.

The objective of the calibration was to obtain a set of parameters that could describe the NH_4^+, NO_2^-, NO_3^- and DO profiles before simulating the associated N_2O production.

The nitrifying fraction of the mixed liquor was calculated from thermodynamics to be 4.1% AOB and 1.8% NOB of the active biomass (SI_1). These results are in agreement with FISH results from other Danish wastewater treatment plants with the same configuration (AOB = 3-5%, NOB = 2.5-3%) (Mielczarek, 2012). Moreover, 16S rRNA-based qPCR quantification of dominant AOB and NOB taxa over 11 weeks showed no variation of the nitrifying community (78 ± 5% AOB/(AOB+NOB), n = 8).

NOB affinity constants differ significantly between species (Nowka et al., 2014), thus NOB affinities were considered as those of *Nitrospira spp*. (Manser et al., 2005) (*Nitrospira spp.* 92 ± 3% relative abundance in comparison to 8 ± 3% of *Nitrobacter spp*.). Results from experiments (i) allowed for estimation of the DO affinity for the first

nitrification step ($K_{O2,AMO}^{AOB}$ = 0.4 mg/L), and the NH_4^+ affinity (K_{NH4}^{AOB} 0.25 mgN/L) (Figure S4). The model could describe hydrolysis and ammonification with default parameter values (Figure S2). Finally, autotrophic maximum specific growth rates (μ_{AMO}^{AOB}, μ^{NOB}) were estimated with low uncertainty (Table II). After model calibration a good individual fitting of DO, NH_4^+, NO_2^- and NO_3^- was obtained ($R^2 > 0.97$, $n > 30$) (Figure 1, left).

3.4.Modelling N_2O production from mixed cultures in autotrophic batch tests.

We analysed the capabilities of the model structures considered (NN, ND, HD, NN-HD, ND-HD) to describe experiments (ii). For each of the five models the best-fit residuals of the N_2O-associated parameter subsets are shown in Table III. Results for the models with the HD_a parameter subset are described below.

(NN): *The nitrifying nitrification pathway (NN) describes N_2O production as a fraction of the oxidized NH_4^+*. The NN model does not consider an effect of NO_2^- on the N_2O produced, and it cannot predict the net N_2O production increase after NO_2^- addition (Figure 2C). The best-fit obtained clearly did not follow the observed N_2O data (Figure 3) (E_{NN} = 0.83).

(ND): The nitrifying denitrification pathway (ND) could describe the observed N_2O responses to substrate concentration changes (E_{ND} = 0.98). The best-fit parameter subset increased the NO_2^- and NO reduction processes with a higher anoxic reduction factor (Table III). The sensitivity of N_2O production to NO_2^- can be described with a low NO_2^- affinity (Figure 3).

(HD): Heterotrophic denitrification processes were limited by the organic substrate (S_S) and DO inhibited. However, an adequate fit could be obtained (E_{HD} = 0.98). Compared

to the initial parameter values the NOR process increased its rate compared to NIR and NOS, indicating a faster NO-to-N_2O turnover (higher μ_{NOR}, $K^{HB}_{NOR,i,O2}$, lower $K^{HB}_{NOR,S}$).

(NN – HD): *The NN-HD model considered the simultaneous NN and HD associated N_2O production.* The best fit of the NN-HD model ($E_{NN\text{-}HD}$ = 0.97) was obtained when the NN contribution to the total N_2O pool was the lowest. This result is in agreement with the fact that NN-associated N_2O production could not describe the data while HD-associated could (E_{NN} = 0.83 vs. E_{HD} = 0.98). Nonetheless, the best-fit was slightly worse than the HD model and better than the NN (Figure 3).

(ND – HD): In the ND-HD model the autotrophic and heterotrophic denitrification pathways were considered and yielded the best fit ($E_{ND\text{-}HD}$ = 0.99). The observed oxygen-inhibited and NO_2^--associated N_2O production could be best described by two independent reductive processes.

The N_2O production rates associated to excess DO were much lower, and lasted shorter periods than N_2O production under DO-limiting conditions (Figure 2). For this reason, models containing one or two denitrification pathways (ND, HD, NN-HD, ND-HD) yielded a better fit than the one associated only with NH_4^+ oxidation (NN). Hence, models containing at least one denitrification pathway obtained very similar fits but suggested different N_2O pathway contributions (N_2O_{ND}, N_2O_{HD} = 0-100%) (Figure 3, Figure S5).

3.5.Influence of HD on N_2O modelling results.

The best N_2O fit was obtained when two simultaneous denitrification processes were considered (ND-HD) regardless of the HD parameter subset chosen (Table III, Table SVII). Even though the total N_2O production was described equally well by ND-HD_a

and ND-HD_b, other model outputs showed very different results (Table IV). Surprisingly, HD was suggested as the main contributor to the total N_2O pool: 96% $N_2O_{HD\_a}/N_2O_{TOT}$ and 61% $N_2O_{HD\_b}/N_2O_{TOT}$. The total NO emitted predicted by the ND-HD models also showed significant differences (0.2 and 10.5% NO/N_2O for ND-HD_a and ND-HD_b). Hence, the model could describe the total N_2O production but neither the individual N_2O pathway contribution nor NO emissions.

4. Discussion

4.1.Predicting capabilities of N_2O model structures.

The best-fit obtained for the N_2O profiles in experiments (ii) varied considerably among the models considered. However, because of the low N_2O emission factor, all the N_2O models in this study could describe NH_4^+, NO_2^-, NO_3^- and DO profiles.

Single pathways

In the NN model, N_2O production is directly linked to NH_2OH oxidation. The initial N_2O production after an NH_4^+ spike can be described by a high concentration of electron donors and electron acceptors (Figure 2, t < 20 min). Even though the NN model could not predict the observed N_2O production at limiting DO and as a response to NO_2^- changes (Figure 2C), it was suitable for non-limiting DO conditions (Ni et al., 2013b; Peng et al., 2015b). The ND model captured the observed N_2O data, suggesting complete autotrophic N_2O production. The larger production of N_2O at low DO and high NO_2^- was captured by changes in oxygen inhibition ($K_{i,O2}^{AOB}$) and NO_2^- affinity (K_{NO2}^{AOB}) from their literature values.

Interestingly, the HD model also captured the N_2O produced suggesting complete heterotrophic N_2O production. Even at conditions of minimum C/N and in the presence of inhibitory DO concentrations for heterotrophic denitrification the best-fit obtained for

the ND and HD models were similar (E_i = 0.98). It should be highlighted that not considering hydrolysis, the only carbon source in these experiments, would have neglected the possible heterotrophic contribution.

Combined pathways

In the NN-HD model, the best-fit results suggest a high HD (N_2O_{HD} = 90%) and small NN (N_2O_{NN} = 10%) contribution to the total N_2O pool as the NN pathway is independent of NO_2^- levels. Both autotrophic and heterotrophic pathways consider N_2O production from NO reduction, thus allowing NN-associated N_2O production to occur even at low DO regardless of NO's producer. The predictions obtained using the ND-HD model yielded the best fit (E_i > 0.99) by combining two denitrification pathways and suggested a very low autotrophic contribution (N_2O_{ND} = 4%). Shen et al. (2014) also suggested that N_2O production during nitrification could be significantly affected by the microbial competition with heterotrophic activity (Shen et al., 2015). As two denitrification processes, ND and HD have similar affinities for N-substrate and DO. Moreover, the organic carbon limitation of heterotrophs under low C/N is counteracted by a larger fraction of the microbial community in mixed liquor. ND and HD can therefore co-occur at similar conditions and rates, which difficult the identifiability of individual pathways solely with bulk N_2O measurements.

Hence, one cannot ignore heterotrophic contribution to N_2O even during a short batch test where the only carbon source was released from hydrolysis of decay products. This is illustrated by two different combined ND-HD models that could best describe the observed data with parameter values within literature range.

Spérandio *et al.* (2016) compared five N_2O models (HD + NN or ND) to four long-term dataseries (Spérandio et al., 2016). The relative contribution of autotrophs (ND) and

heterotrophs (HD) to the total N_2O production was calculated for a full-scale UCT process. For every 3 units of N_2O produced by the ND pathway 2 were consumed by HD, highlighting the importance of including the HD under AOB-driven N_2O production.

The better performance of multiple-pathway models suggests that new and more complex models will be necessary to predict N_2O emissions from dynamic systems (Spérandio et al., 2016). Considering additional pathways increases their fitting capabilities but, as highlighted in this study, our understanding of simple models is still limited. Moreover, overparameterization might compromise the precision and identifiability of complex models, which has not been critically addressed yet. This will support the model discrimination procedure towards developing a new biologically congruent N_2O model.

4.2. Limitations of modelling combined N_2O production pathways from bulk N_2O measurements.

The aim of modelling biological N_2O production during wastewater treatment operations is to mitigate its emissions by understanding how operating conditions relate to N_2O production. The desired mitigation strategies of N_2O models are specific to the main producing pathway. If the production of each pathway is accounted for individually we can better understand the relevant N_2O producing processes (Ni et al., 2014). However, because no direct pathway measurements are possible, model predictions are considered instead. N_2O models are usually calibrated with N_2O bulk measurements (liquid or gas phase), from which the contribution of each pathway is calculated (Guo and Vanrolleghem, 2013; Ni et al., 2014). The uncertainty associated to

model predictions can be calculated by mapping input uncertainty (error in parameter estimates) onto model outputs.

The high variability found in N_2O model parameters was studied in the ND-HD model by varying one parameter commonly fixed (K_{NO}^{AOB}, K_{NO}^{HB}) within literature range (Hiatt and Grady, 2008; Spérandio et al., 2016). Because the total N_2O production is not sensitive to these parameters (data not shown) no effect is seen in the model output for experiments (ii) (Figure 4, Figure S6). However, variables such as the autotrophic N_2O contribution or the total NO production can vary significantly (Figure 4A,B). These results indicate that fixing K_{NO} values from literature values can lower model predicting capabilities for individual N_2O pathway contributions based on calibrations from N_2O bulk measurements.

NO plays an important role in N_2O production as its precursor in every production pathway (HD, ND, NN) and can, under certain conditions, contribute more than N_2O to the nitrogen loss (Castro-Barros et al., 2016). In experiments (ii), measuring NO would help to elucidate the main NO and N_2O production pathways by not lumping NO_2^- and NO reduction processes, an assumption made by new N_2O models (Ni et al., 2014; Pocquet et al., 2016). For a combination of K_{NO}^{AOB} and K_{NO}^{HB} values the model output for NO and N_2O is shown in Figure 5. The total error of N_2O production, shown as RMSE, does not vary regardless of the K_{NO}^{AOB}-K_{NO}^{HB} values (Figure 5A). On the other hand, both the contribution of the autotrophic pathway (Figure 5B) and the total NO produced (Figure 5C) vary significantly (1-56% $N_2O_{AOB}/N_2O_{TOT,}$ 0.2-4.0% NO/N_2O). Thus, because NO is more sensitive to K_{NO} than N_2O is, NO data availability will increase the identifiability of K_{NO}^{AOB}-K_{NO}^{HB}. Consequently, the contribution of each N_2O production pathway can be estimated more accurately. This is in agreement with the suggestion of

Spérandio et al. (2016) of using the ratio NO/N_2O as a parameter for model discrimination (Spérandio et al., 2016).

5. Conclusions

In this work, N_2O production from nitrifying batch experiments with mixed liquor was studied experimentally and compared to predictions by five model structures. Contrary to our hypothesis even under very low C/N conditions heterotrophic activity was found comparable to autotrophic nitrification activity in terms of N_2O production. Interestingly, process models accounting for heterotrophic and autotrophic denitrification pathways could describe total N_2O profiles only slightly better than single-pathway denitrification models. In a conventional N-removing system, where heterotrophs are more abundant than autotrophs, different combinations of denitrification N_2O-producing pathways could describe the observed biological N_2O production. Thus, based on N_2O bulk measurements from mixed liquor, models cannot unambiguously elucidate the contribution of each N_2O production pathway due to parameter uncertainty.

Acknowledgements

This research was funded by the Danish Agency for Science, Technology and Innovation through the Research Project LaGas (12-132633). The authors have no conflict to declare.

References

Ahn JH, Kim S, Park H, Rahm B, Pagilla K, Chandran K. 2010. N2O emissions from activated sludge processes, 2008-2009: results of a national monitoring survey in the United States. *Environ. Sci. Technol.* **44**:4505–11.

APHA, AWWA, WEF. 1999. Standard Methods for the Examination of Water and Wastewater. Ed. American Public Health Association 20th ed. Washington DC.

Castro-Barros C, Rodríguez-Caballero A, Volcke EIP, Pijuan M. 2016. Effect of nitrite on the N2O and NO production on the nitrification of low-strength ammonium wastewater. *Chem. Eng. J.* **287**:269–276.

Dochain D, Vanrolleghem PA. 2001. Dynamic Modelling and Estimation in Wastewater Treatment Processes. London, UK: IWA Publishing.

Domingo-Félez C, Mutlu a G, Jensen MM, Smets BF. 2014. Aeration Strategies To Mitigate Nitrous Oxide Emissions from Single-Stage Nitritation/Anammox Reactors. *Environ. Sci. Technol.* **48**:8679–8687.

Ellis TG, Barbeau DS, Smets BF, Grady CPL. 1996. Respirometric technique for determination of extant kinetic parameters describing biodegradation. *Water Environ. Res.* **68**:917–926.

Garcia-Ochoa F, Gomez E. 2009. Bioreactor scale-up and oxygen transfer rate in microbial processes: an overview. *Biotechnol. Adv.* **27**:153–76.

Guo L, Vanrolleghem P a. 2013. Calibration and validation of an activated sludge model for greenhouse gases no. 1 (ASMG1): prediction of temperature-dependent N2O emission dynamics. *Bioprocess Biosyst. Eng.* **1**.

Gustavsson DJI, Tumlin S. 2013. Carbon footprints of Scandinavian wastewater treatment plants. *Water Sci. Technol.* **68**:887.

Hauduc H, Rieger L, Takács I, Héduit A, Vanrolleghem PA, Gillot S. 2010. A systematic approach for model verification: application on seven published activated sludge models. *Water Sci. Technol.* **61**:825–39.

Hiatt WC, Grady CPL. 2008. An updated process model for carbon oxidation, nitrification, and denitrification. *Water Environ. Res.* **80**:2145–2156.

Itokawa H, Hanaki K, Matsuo T. 2001. Nitrous oxide production in high-loading biological nitrogen removal process under low COD/N ratio condition. *Water Res.* **35**:657–664.

Jiang D, Khunjar WO, Wett B, Murthy SN, Chandran K. 2015. Characterizing the Metabolic Trade-Off in Nitrosomonas europaea in Response to Changes in Inorganic Carbon Supply. *Environ. Sci. Technol.* **49**:2523–31.

Kampschreur MJ, Picioreanu C, Tan N, Kleerebezem R, Jetten MS., van Loosdrecht MC. 2007. Unraveling the Source of Nitric Oxide Emission During Nitrification. *Water Environ. Res.* **79**:2499–2509.

Kampschreur MJ, Temmink H, Kleerebezem R, Jetten MSM, van Loosdrecht MCM. 2009. Nitrous oxide emission during wastewater treatment. *Water Res.* **43**:4093–103.

Khunjar WO, Jiang D, Murthy S, Wett B, Chandran K. 2011. Linking the Nitrogen and One-Carbon Cycles - The Impact of Inorganic Carbon Limitation on Ammonia Oxidation and Nitrogen Oxide Emission Rates in Ammonia Oxidizing

Bacteria:3199–3207.

Law Y, Ye L, Pan Y, Yuan Z. 2012. Nitrous oxide emissions from wastewater treatment processes. *Philos. Trans. R. Soc. Lond. B. Biol. Sci.* **367**:1265–77.

Mampaey KE, Beuckels B, Kampschreur MJ, Kleerebezem R, van Loosdrecht MCM, Volcke EIP. 2013. Modelling nitrous and nitric oxide emissions by autotrophic ammonia-oxidizing bacteria. *Environ. Technol.* **34**:1555–1566.

Mannina G, Cosenza A, Vanrolleghem PA, Viviani G. 2011. A practical protocol for calibration of nutrient removal wastewater treatment models. *J. Hydroinformatics* **13**:575.

Manser R, Gujer W, Siegrist H. 2005. Consequences of mass transfer effects on the inetics of nitrifiers. *Water Res.* **39**:4633–42.

Mielczarek AT. 2012. Microbial Communities in Danish Wastewater Treatment Plants with Nutrient Removal; Aalborg University, Denmark.

Monteith HD, Sahely HR, MacLean HL, Bagley DM. 2005. A Rational Procedure for Estimation of Greenhouse-Gas Emissions from Municipal Wastewater Treatment Plants. *Water Environ. Res.* **77**:390–403.

Ni B-J, Peng L, Law Y, Guo J, Yuan Z. 2014. Modeling of Nitrous Oxide Production by Autotrophic Ammonia-Oxidizing Bacteria with Multiple Production Pathways. *Environ. Sci. Technol.* **48**:3916–24.

Ni B-J, Ruscalleda M, Pellicer-Nàcher C, Smets BF. 2011. Modeling nitrous oxide production during biological nitrogen removal via nitrification and denitrification: extensions to the general ASM models. *Environ. Sci. Technol.* **45**:7768–76.

Ni B-J, Ye L, Law Y, Byers C, Yuan Z. 2013a. Mathematical modeling of nitrous oxide (N2O) emissions from full-scale wastewater treatment plants. *Environ. Sci. Technol.* **47**:7795–803.

Ni B-J, Yuan Z, Chandran K, Vanrolleghem P a., Murthy S. 2013b. Evaluating four mathematical models for nitrous oxide production by autotrophic ammonia-oxidizing bacteria. *Biotechnol. Bioeng.* **110**:153–63.

Nowka B, Daims H, Spieck E. 2014. Comparative oxidation kinetics of nitrite-oxidizing bacteria: nitrite availability as key factor for niche differentiation. *Appl. Environ. Microbiol.* **81**:745–753.

Pan Y, Ni B, Yuan Z. 2013. Modeling electron competition among nitrogen oxides reduction and N2O accumulation in denitrification. *Environ. Sci. Technol.* **47**:11083–91.

Peng L, Ni B-J, Ye L, Yuan Z. 2015a. N2O production by ammonia oxidizing bacteria in an enriched nitrifying sludge linearly depends on inorganic carbon concentration. *Water Res.* **74**:58–66.

Peng L, Ni B-J, Ye L, Yuan Z. 2015b. Selection of mathematical models for N2O production by ammonia oxidizing bacteria under varying dissolved oxygen and nitrite concentrations. *Chem. Eng. J.* **281**:661–668.

Perez-Garcia O, Villas-Boas SG, Swift S, Chandran K, Singhal N. 2014. Clarifying the regulation of NO/N2O production in Nitrosomonas europaea during anoxic-oxic transition via flux balance analysis of a metabolic network model. *Water Res.* **60C**:267–277.

Pocquet M, Wu Z, Queinnec I, Spérandio M. 2016. A two pathway model for N2O emissions by ammonium oxidizing bacteria supported by the NO/N2O variation. *Water Res.* **88**:948–959.

Reichert P. 1998. AQUASIM 2.0 - User Manual. Computer Program for the Identification and Simulation of Aquatic Systems. Swiss Federal Institute for Environmental Science and Technology (EAWAG).

Schreiber F. 2009. Mechanisms of Transient Nitric Oxide and Nitrous Oxide Production in a Complex Biofilm_SI. *ISME J.*:1–8.

Schreiber F, Wunderlin P, Udert KM, Wells GF. 2012. Nitric oxide and nitrous oxide turnover in natural and engineered microbial communities: biological pathways, chemical reactions, and novel technologies. *Front. Microbiol.* **3**:372.

Schulthess R Von, Wild D, Gujer W. 1994. Nitric and nitrous oxides from denitrifying activated sludge at low oxygen concentration. *Water Sci. Technol.* **30**:123–132.

Shen L, Guan Y, Wu G. 2015. Effect of heterotrophic activities on nitrous oxide emission during nitrification under different aeration rates. *Desalin. Water Treat.* **55**:821–827.

Spérandio M, Pocquet M, Guo L, Ni BJ, Vanrolleghem PA, Yuan Z. 2016. Evaluation of different nitrous oxide production models with four continuous long-term wastewater treatment process data series. *Bioprocess Biosyst. Eng.*

Stocker TF, Qin D, Plattner G-K, Tignor M, Allen SK, Boschung J, Nauels A, Xia Y, Bex V, Midgley PM. 2013. IPCC Fifth Assessment Report - The physical science basis. *IPCC*. Cambridge, United Kingdom and New York, NY, USA: Cambridge University Press 1535 p.

Terada A, Lackner S, Kristensen K, Smets BF. 2010. Inoculum effects on community composition and nitritation performance of autotrophic nitrifying biofilm reactors with counter-diffusion geometry. *Environ. Microbiol.* **12**:2858–2872.

Torà J a, Lafuente J, Baeza J a, Carrera J. 2010. Combined effect of inorganic carbon limitation and inhibition by free ammonia and free nitrous acid on ammonia oxidizing bacteria. *Bioresour. Technol.* **101**:6051–8.

Wu G, Zhai X, Li B, Jiang C, Guan Y. 2014. Endogenous Nitrous Oxide Emission for Denitrifiers Acclimated with Different Organic Carbons. *Procedia Environ. Sci.* **21**:26–32.

Heterotrophs are key contributors to nitrous oxide production in mixed liquor under low C-to-N ratios during nitrification – batch experiments and modelling

Author list

Carlos Domingo-Félez[1], Carles Pellicer-Nàcher[1], Morten S. Petersen[1], Marlene M. Jensen[1], Benedek G. Plósz[1], Barth F. Smets[1]*

[1]Department of Environmental Engineering, Technical University of Denmark, Miljøvej 113, 2800 Kgs. Lyngby, Denmark

* Corresponding author:

Barth F. Smets, Phone: +45 4525 1600, Fax: +45 4593 2850, E-mail: bfsm@env.dtu.dk

Running title: N_2O production in nitrifying batch experiments: heterotrophic and autotrophic contributions.

List of Figures

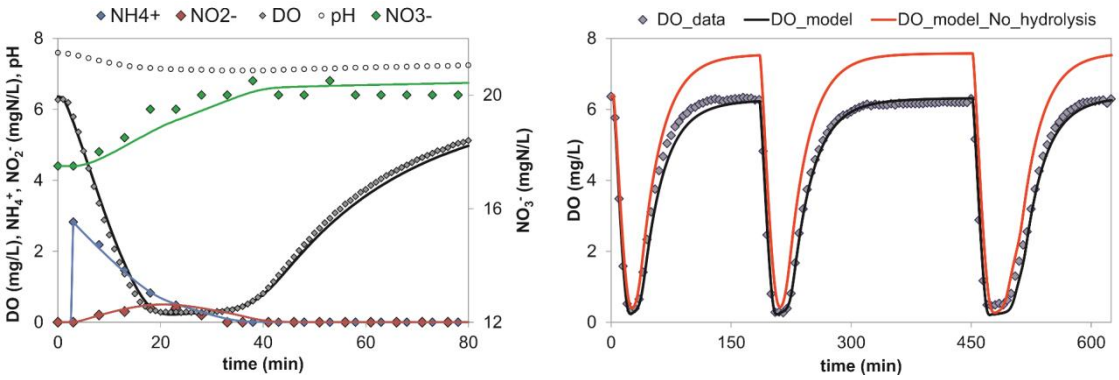

Figure 1 – Left: Concentration profile in a batch experiment after an NH_4^+ spike (experimental data: markers, model: lines). Right: Comparison between measured DO concentrations (diamonds) and model-predicted results when decay and hydrolysis are considered (black line) or neglected (red line).

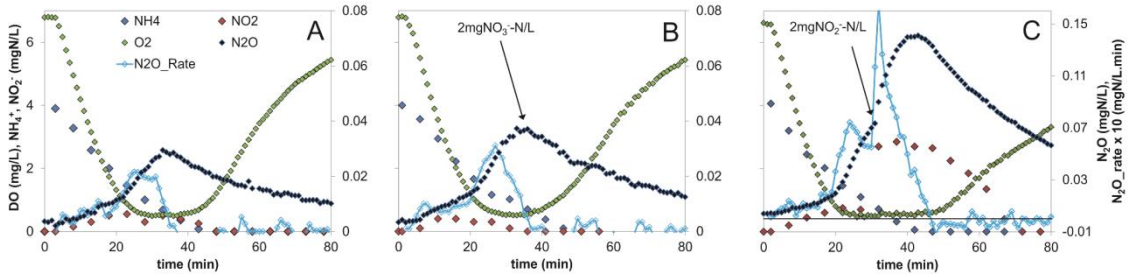

Figure 2 – N_2O production during batch tests (ii): NH_4^+ spike (A), NH_4^+ spike followed by NO_3^- spike (B), NH_4^+ spike followed by NO_2^- spike (C).

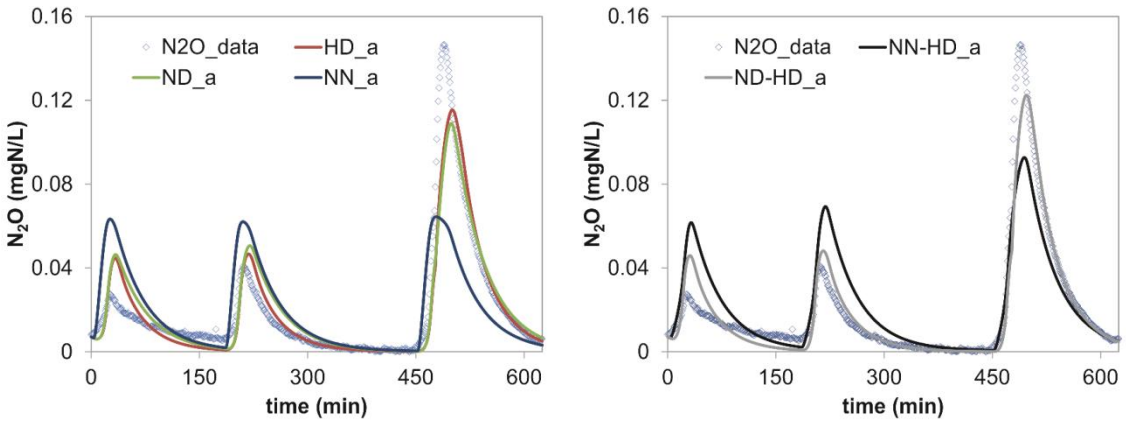

Figure 3 – Experimental and best-fit simulations of N_2O concentrations during experiments (i). Individual pathways: HD, ND, NN (left); and combined pathways: ND-HD, NN-HD (right). Parameter subset HD_a.

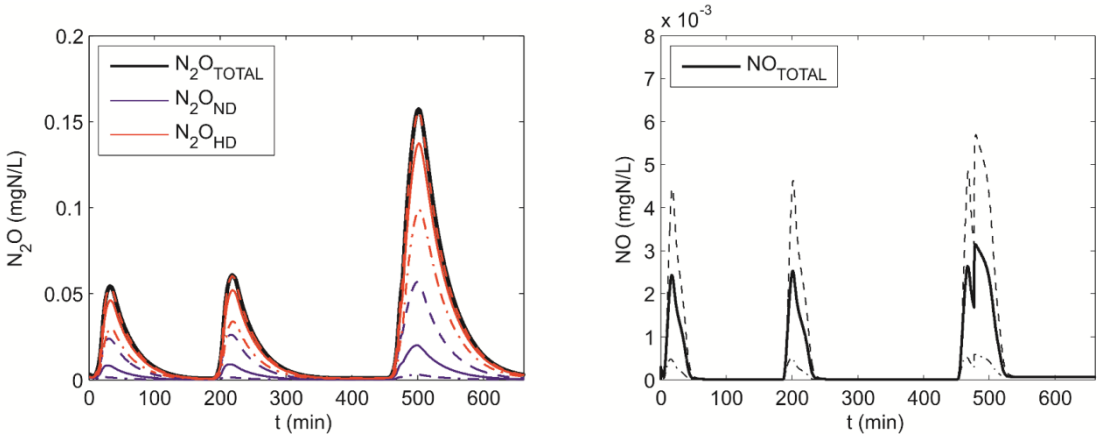

Figure 4 – Modelling results for ND-HD_a best-fit parameters in experiment (ii) (Table III). 250 $K_{NO(AOB,\ HB)}$ pairs of values sampled randomly in the range 0.02 ± 90% mgN/L. Total contribution (black) and decomposed HD (red) and ND (blue) individual contributions and to the N_2O pool (left). Total NO production (right). Dashed lines correspond to the 95% percentiles.

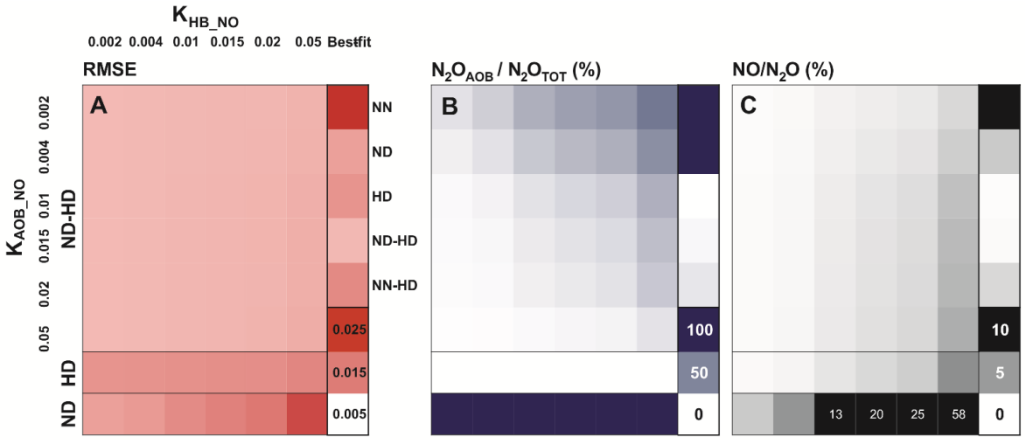

Figure 5 – Results of model simulations. Left panels: varying K_{NO} values (0.002 – 0.05 mgN/L) for the ND-HD model (K_{HB_NO}, K_{AOB_NO}), HD model (K_{HB_NO}) and ND model (K_{AOB_NO}). Right panels: Best-fit results for NN, ND, HD, NN-HD and ND-HD models. Parameter subset HD_a.

(A) N_2O fit (RMSE), (B) autotrophic contribution to the total N_2O pool, (C) NO/N_2O produced.

Heterotrophs are key contributors to nitrous oxide production in mixed liquor under low C-to-N ratios during nitrification – batch experiments and modelling

Author list

Carlos Domingo-Félez[1], Carles Pellicer-Nàcher[1], Morten S. Petersen[1], Marlene M. Jensen[1], Benedek G. Plósz[1], Barth F. Smets[1]*

[1]Department of Environmental Engineering, Technical University of Denmark, Miljøvej 113, 2800 Kgs. Lyngby, Denmark

* Corresponding author:
Barth F. Smets, Phone: +45 4525 1600, Fax: +45 4593 2850, E-mail: bfsm@env.dtu.dk

Running title: N_2O production in nitrifying batch experiments: heterotrophic and autotrophic contributions.

Tables

Table I – Combination of N_2O-producing model structures considered.

Scenario	Nitrif. Nitrification	Nitrif. Denitrification	Heter. Denitrification
NN	✓		2 step (no N_2O)
ND		✓	2 step (no N_2O)
HD			✓ 4 step (a / b)
NN-HD	✓		✓ 4 step (a / b)
ND-HD		✓	✓ 4 step (a / b)

Heterotrophic denitrification (HD) is modelled with two different parameter subsets (a) and (b).

Table II – Best-fit parameter estimates during NH_4^+, NO_2^-, NO_3^- and DO calibration.

	Initial	Best-fit_a	Best-fit_b
u_{AMO} (h^{-1})	0.205	0.182 ± 0.0019	0.187 ± 0.0023
u_{NOB} (h^{-1})	0.060	0.015 ± 0.0001	0.015 ± 0.0001
Correlation		0.51	0.55

Table III – Best-fit estimates of N2O-related parameters for each model structure considered (HD_a).

			NN	ND	HD	NN-HD	ND-HD	Lit. Range	Ref.
η_{AOB}	Anoxic reduction factor	(-)	0.28	0.56		0.06	0.56	0.053 - 0.5	(1) (2) (3) (4)
$K_{AOB\ NO2}$	NO_2^- affinity coefficient for denitrification	(mgN/L)		0.61			0.8*	0.14 - 8	(5) (6) (7) (8)
$K_{AOB\ i\ O2}$	O_2 inhibition coefficient for denitrification	(mgCOD/L)		0.15			0.15	0.078 - 0.112	(1) (2) (3) (4)
u_{NIR}	Max. NO_2^- reduction rate	(h^{-1})			0.055	0.098	0.059	0.017 - 0.078	(3) (9) (10) (11)
u_{NOR}	Max. NO reduction rate	(h^{-1})			0.213	0.213	0.137	0.038 - 0.345	(1) (3) (10) (11)
u_{NOS}	Max. N_2O reduction rate	(h^{-1})			0.077	0.079	0.125	0.065 - 0.182	(3) (9) (10) (11)
$K_{HB\ i\ O2\ NIR}$	O_2 inhibition coefficient for NO_2^- denitrification	(mgCOD/L)			0.05	0.13	0.05	0.1 - 1	(9) (10) (11)
$K_{HB\ i\ O2\ NOR}$	O_2 inhibition coefficient for NO denitrification	(mgCOD/L)			0.10	0.03	0.10	0.067 - 1	(1) (3) (10) (11)
$K_{HB\ i\ O2\ NOS}$	O_2 inhibition coefficient for N_2O denitrification	(mgCOD/L)			0.03	0.05	0.02	0.031 - 1	(9) (10) (11)
$K_{HB\ S\ NIR}$	S_S affinity coefficient for NO_2^- denitrification	(mgCOD/L)			0.8	0.8	1.8	1.5 - 20	(9) (10) (11)
$K_{HB\ S\ NOR}$	S_S affinity coefficientfor NO denitrification	(mgCOD/L)			1.2	1.2	1.2	0.56 - 20	(1) (3) (10) (11)
$K_{HB\ S\ NOS}$	S_S affinity coefficient for N_2O denitrification	(mgCOD/L)			3.0	3.0	3.0	2 - 40	(9) (10) (11)
Best-fit	E_{N2O}		0.83	0.98	0.98	0.97	0.99		
	RMSE		0.022	0.012	0.013	0.014	0.010		

(1) - Ni *et al.* 2011, (2) - Ni et al. 2013a, (3) Ni et al. 2013b, (4) Spérandio et al. 2016, (5) Schreiber et al. 2009, (6) Kampschreur et al. 2008, (7) Mampaey et al. 2013, (8) Garnier et al. 2007, (9) von Schulthess et al. 1994, (10) Guo et al. 2013, (11) Hiatt and Grady 2008. * Fixed value

Table IV – Modelling results for the ND-HD model.

		ND-HD_a	ND-HD_b
E_i	(-)	0.993	0.995
N_2O_{AOB}/TOT	(%)	4	39
NO/N_2O	(%)	0.2	10.5
NO_{AOB}/TOT	(%)	67	37
N_2	(mgN/L)	0.19	0.39